Optical spectra of Nd^{3+} in niobates of the tetragonal tungsten bronze family

2004 J. Phys.: Condens. Matter 16 729

(http://iopscience.iop.org/0953-8984/16/6/004)

INSTITUTE OF PHYSICS PUBLISHING JOURNAL OF PHYSICS: CONDENSED MATTER

J. Phys.: Condens. Matter **16** (2004) 729–739 PII: S0953-8984(04)68700-5

Optical spectra of Nd^{3+} in niobates of the tetragonal tungsten bronze family

Enrico Cavalli[1,3], Gianluca Calestani[1], Enrico Bovero[1], Alessandro Belletti[1] and Andrea Migliori[2]

[1] INFM and Dipartimento di Chimica Generale ed Inorganica, Chimica Analitica e Chimica Fisica, Università di Parma, Viale delle Scienze 17/a, 43100 Parma, Italy
[2] CNR-IMM, Sezione di Bologna, Via P Godetti 101, 40129 Bologna, Italy

E-mail: enrico.cavalli@unipr.it

Received 8 September 2003
Published 30 January 2004
Online at stacks.iop.org/JPhysCM/16/729 (DOI: 10.1088/0953-8984/16/6/004)

Abstract

$Nd:Ba_2NaNb_5O_{15}$ (Nd:BNN), $Nd:Ba_2KNb_5O_{15}$ (Nd:BKN) and $Ba_{1.90}Nd_{0.26}Li_{0.42}Nb_5O_{15}$ (BNdLN) single crystals with the tetragonal tungsten–bronze (TTB) structure have been grown by means of the 'flux growth' method. The 10 and 298 K absorption and emission spectra and the room temperature decay curves have been measured and discussed in the light of the crystallographic information. The room temperature absorption spectra of Nd:BKN and BNdLN have been analysed in the framework of Judd–Ofelt theory and the Ω_λ ($\lambda = 2$, 4, 6) intensity parameters have been evaluated. The structural and emission properties of a new TB phase, $Nd:Ba_2LiNb_5O_{15}$ (Nd:BLN), have also been reported because they are useful in the discussion concerning the site occupancy of the active ions in these materials.

1. Introduction

Niobates with the tetragonal tungsten–bronze (TTB) structure belong to a large family of compounds having interesting ferroelectric, nonlinear and electro-optical properties [1]. $Ba_2NaNb_5O_{15}$ (BNN), for example, has been extensively studied for more than 30 years in order to develop new materials for optical and laser applications [2, 3]. The growth of single crystals of TTB niobates is not easy [4, 5] and constitutes a serious drawback to their characterization and application. In a series of 'flux growth' experiments in the B_2O_3–Nb_2O_5–BaO–Nd_2O_3–M_2O (M = Li, Na, K) system we have obtained a number of different phases. Among these, single crystals of Nd:BNN, $Nd:Ba_2LiNb_5O_{15}$ (Nd:BLN), $Nd:Ba_2KNb_5O_{15}$ (Nd:BKN), $Ba_{1.90}Nd_{0.26}Li_{0.42}Nb_5O_{15}$ (BNdLN) and $K_2NdNb_5O_{15}$ (KNdN) suitable for crystallographic and optical measurements were isolated. In this paper we

[3] Author to whom any correspondence should be addressed.

report on the spectroscopic properties of the tetragonal Nd:BNN, BNdLN and Nd:BKN crystals. Although the optical spectra of Nd:BNN have been already investigated by different authors [3, 4, 6], some new results will be presented here. They are, in our opinion, important in order to understand the nature of the optical centres in these materials. The 10 and 298 K absorption and emission spectra and the room temperature decay curves have been measured and discussed in the light of the structural data obtained from x-ray diffraction (XRD) experiments. The Judd–Ofelt (JO) intensity parameters have been determined for BNdLN and Nd:BKN from analysis of the room temperature absorption spectra and used to calculate the radiative lifetimes of the emitting levels. These values have then been compared with those obtained from the experimental decay curves in order to estimate the efficiencies of the nonradiative processes. The emission spectra of Nd:BLN will also be presented because they are useful for understanding the relationship between structural and optical properties in these compounds.

2. Experimental details

The crystals were grown by means of the 'flux growth' method, consisting of the slow cooling of suitable molten salt solutions. High purity BaO, B_2O_3, Nb_2O_5, Nd_2O_3 and M_2CO_3 (M = Li, Na, K) were used as starting materials. The growth mixtures were put in platinum crucibles with tight fitting lids and the syntheses were carried out in a programmable furnace. Several experiments were performed with different starting compositions and thermal programmes in order to assess the best conditions for the growth of the crystals of interest. Different phases have been isolated and identified, some of them for the first time. The details of crystal growth and of the crystal structure analyses will be given in a future paper. Blue Nd:BNN (with two different Nd^{3+} concentrations), BNdLN and Nd:BKN crystals, with sizes up to $3 \times 2 \times 2$ mm^3 and good optical quality, were grown by this method. Smaller, almost colourless, Nd:BLN crystals were obtained from the same batch of BNdLN; their quality was quite poor but sufficient for emission measurements. Some preliminary results, useful for the interpretation of the spectroscopic data, are reported in the next section. Structural characterizations were performed by single-crystal x-ray diffraction by using a Philips PW1100 diffractometer. Intensity data were collected with Mo Kα radiation, θ–2θ scan, 3°–45° θ range. The structures were solved by SIR97 [7] and refined with SHELX-97 [8]. Transmission electron microscopy (TEM) techniques, in particular selected-area electron diffraction (SAED) and high resolution electron microscopy (HREM), have been associated with XRD techniques in the resolution of the crystallographic problems.

The absorption spectra were recorded in the 400–900 nm range using a spectroscopic system made up of a 300 W halogen lamp fitted with a 0.22 Spex minimate monochromator as the source and a 1.26 m Spex monochromator with a RCA C31034 photomultiplier to analyse and detect the output radiation. The incident light was polarized by means of two calcite Glan–Thomson prisms placed both in the sample and in the reference beam. The same set-up, properly modified, was used to measure the luminescence spectra. The emission spectra in the 850–1150 nm range were excited at 514 nm using an Ar^+ laser (ILT6500AWC-00) or at 575 nm using a filtered 450 W Xe lamp. A NIR extended photomultiplier (EMI TE9684QB) was used to detect the emission output. For the fluorescence decay curve measurements, the samples were excited at 740 nm using a Quanta System Ti–sapphire pulsed laser system, the emission was isolated by means of a Hilger–Watts Model D330 double monochromator and detected with a Hamamatsu R943-022 photomultiplier connected to a LeCroy 9410 transient digitizer. The samples were cooled by means of a He closed cycle cryostat.

3. Crystallographic data

The TTB structure can be considered as a layered framework of corner linked NbO_6 octahedra in which the cavities, connected in channels running along the stacking axis c, have triangular (C), square (A_2) and pentagonal (A_1) sections in the ab plane. The site labelling has been adopted according to Neurgaonkar and Cory [1], who represented the compositions of the tungsten bronzes by the general formula $(A_1)_4(A_2)_2(C)_4B_{10}O_{30}$. The C sites can be occupied only by ions with small radii (e.g. Li^+) and are often empty, whereas the A_2 and A_1 sites, having 12-fold and 15-fold oxygen coordination, respectively, can be occupied by different cations in variable percentages, depending on the chemical composition and on the sizes of the cations. These cavities are evident in figure 1(a), where a projection of the structure along the crystallographic c axis is shown. Structural studies of the TTB niobates are complicated by several factors, such as the existence of different phase transitions, commensurate or incommensurate modulations and microtwinning resulting in the presence of ferroelectric or ferroelastic domains [9, 10]. SAED studies performed on our samples showed, in agreement with data from the literature, that BNN, BKN and BNdLN structures are affected by quasi-commensurate structural modulation (with a modulation wavevector about four times the (110) direction of the fundamental TTB subcell). This modulation, produced by cooperative tilting of the NbO_6 octahedra, reduces the real symmetry of these systems from tetragonal to orthorhombic. Owing to the extreme weakness of the modulation satellites in XRD and to the presence of ferroelastic twinning that interchanges the a and b axes, the crystal structure analysis, carried out on the basis of single-crystal x-ray diffraction data, was performed in the fundamental tetragonal subcell with the main goal of determining the site occupancy of the different extra-framework cations. In the $P4bm$ space group of TTB the lattice parameters of Nd:BNN are $a = 12.463(1)$ Å and $b = 3.990(1)$ Å, those of BNdLN are $a = 12.441(1)$ Å and $b = 3.971(1)$ Å and those of Nd:BKN are $a = 12.459(1)$ Å and $b = 3.960(1)$ Å. The refinement of the site occupancies indicates that Nd^{3+} is located exclusively at the 12-fold coordinated A_2 site and that A_1 sites are not fully occupied by Ba^{2+}. The C sites of Nd:BNN and BNdLN are, to some extent, occupied by Na^+ or Li^+, in agreement with the electron density residuals found in the ΔF maps. Using the Neurgaonkar $(A_1)_4(A_2)_2(C)_4B_{10}O_{30}$ notation [1] the actual compositions of the crystals can be expressed as follows:

Nd:BNN (dil.) $\leftrightarrow (Ba_{0.95}\square_{0.05})_4(Na_{0.99}Nd_{0.01})_2(\square_{0.91}Na_{0.09})_4Nb_{10}O_{30}$

Nd:BNN (conc.) $\leftrightarrow (Ba_{0.92}\square_{0.08})_4(Na_{0.93}Nd_{0.07})_2(\square_{0.91}Na_{0.09})_4Nb_{10}O_{30}$

BNdLN $\leftrightarrow (Ba_{0.95}\square_{0.05})_4(Nd_{0.26}\square_{0.74})_2(\square_{0.80}Li_{0.20})_4Nb_{10}O_{30}$

Nd:BKN $\leftrightarrow (Ba_{0.90}K_{0.05}\square_{0.05})_4(K_{0.85}Nd_{0.15})_2(\square)_4Nb_{10}O_{30}$

where $\square$ indicates cationic vacancies.

Nd:BLN presents a new type of TB structure, which has never been reported before, to the best of our knowledge. In fact, it belongs to the orthorhombic system, space group $Pnma$ and cell parameters $a = 7.951(1)$ Å, $b = 14.951(2)$ Å and $c = 10.222(1)$ Å. The difference between this structure and that of TTB can be understood by observing the different linking of the Nb_9O_{42} units, shown in figure 1, which causes the disappearance of the perovskite-type A_2 cage in BLN and its substitution by a new 12-fold cage (A_3) occupied by the Nd^{3+} and Li^+ ions. The complete chemical formula is $(Ba)_4(Li_{0.73}Nd_{0.09}\square_{0.18})_2(\square)_4Nb_{10}O_{30}$.

Since the optical spectra have been measured at 10 and 298 K, it is important to consider the possible effects of phase transitions in this temperature range. In the case of Nd:BNN, the phase transitions occurring below 575 K are connected with the ferroelasticity of the system and are determined by tilting waves of the NbO_6 octahedra which produce commensurate or incommensurate modulation along given directions. They can be considered like second-

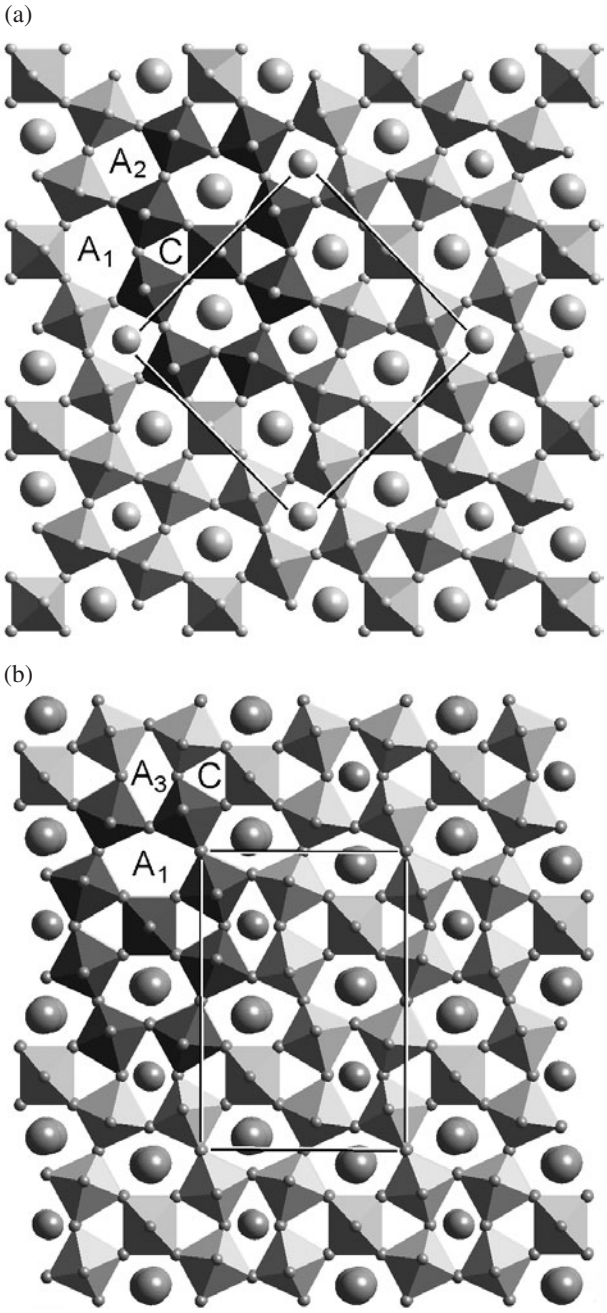

Figure 1. Projection along the *c* axis of the tetragonal tungsten–bronze structure (a) and of the orthorhombic Nd:BLN structure (b).

order transitions which do not imply a significant change in the cell volume and do not appreciably affect the optical spectra. It is reasonable to suppose that the same holds for the other compounds, even if there is no information about their phase transitions, to our knowledge.

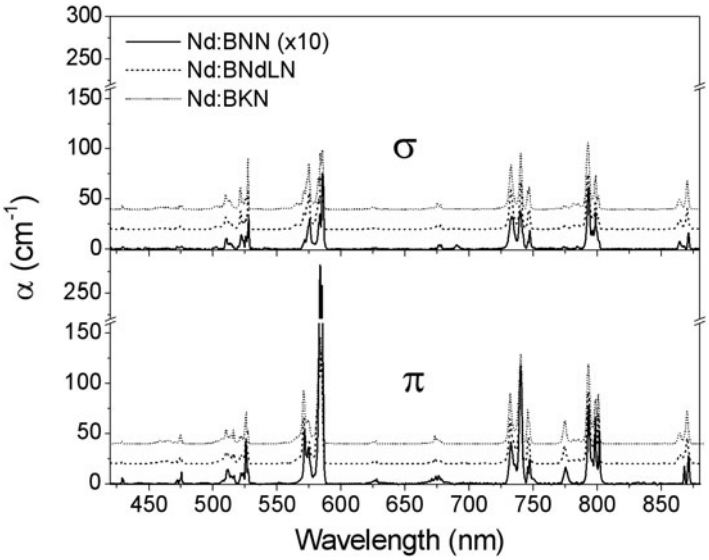

Figure 2. 10 K absorption spectra of Nd:BNN(conc.), BNdLN and Nd:BKN.

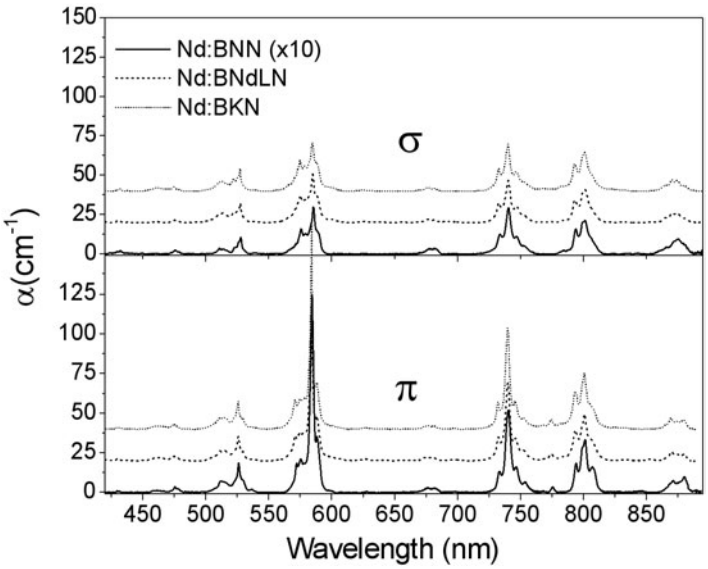

Figure 3. 298 K absorption spectra of Nd:BNN(conc.), BNdLN and Nd:BKN.

4. Results and discussion

The polarized absorption spectra of Nd:BNN, BNdLN and Nd:BKN have been measured at 10 and 300 K for two different configurations: the σ configuration, with the electric field of the incoming beam perpendicular to the c crystal axis of the sample ($E \perp c$), and the π configuration, with the electric field of the incident beam parallel to the c axis ($E \parallel c$). They are shown in figures 2 and 3, respectively. The observed transitions from the $^4I_{9/2}$ ground state to the excited levels of the Nd^{3+} ion have been assigned on the basis of the energy levels scheme

Table 1. Line wavelengths observed in the 10 K absorption spectra.

Final state (no. of theoretical lines)	Nd:BNN	BNdLN	Nd:BKN
$^2D_{5/2}$ (3)	419.6	417.6, 418.8 420.2	418.6, 418.6, 420.2
$^2P_{1/2}$ (1)	429.1, 430.0	429.2	429.1
$^2G_{9/2} + {}^2D_{3/2} + {}^4G_{11/2} + {}^2K_{15/2}$ (21)	471.3, 472.2, 474.4, 475.4	455.0, 457.8, 458.4, 459.6, 463.8, 465.8, 468.8, 471.5, 474.6, 475.8	454.9, 459.6, 463.6, 465.6, 468.7, 471.4, 474.2, 475.9
$^4G_{7/2} + {}^2K_{13/2} + {}^4G_{9/2}$ (16)	507.9, 510.9, 511.6, 513.9, 516.5, 521.9, 523.8, 525.3, 526.1, 527.9	501.8, 507.0, 510.0, 511.4, 513.5, 514.4, 516.2, 521.6, 522.6, 523.6, 525.2, 526.0, 527.4	502.0, 509.8, 511.4, 513.4, 521.3, 523.5, 525.1, 527.2
$^4G_{5/2} + {}^2G_{7/2}$ (7)	571.5, 573.1, 574.5, 575.5, 583.6, 585.0	565.8, 570.8, 573.4, 575.0, 580.6, 582.2, 583.9, 585.4	555.6, 565.4, 570.7, 573.2, 574.6, 582.0, 583.6, 585.2
$^2H_{11/2}$ (6)	624.1, 624.5, 626.4, 627.8	619.6, 624.0, 625.4, 627.2, 629.0	619.6, 623.8, 626.0, 627.0
$^4F_{9/2}$ (5)	668.5, 671.0, 673.8, 676.2, 678.2, 690.0	669.2, 673.2, 675.2, 677.6	669.4, 672.8, 675.0, 677.2
$^4F_{7/2} + {}^4S_{3/2}$ (6)	732.5, 735.6, 740.0, 745.4, 747.2, 750.7	732.0, 732.6, 734.4, 740.2, 746.0, 749.6	732.2, 740.0, 745.4, 746.6
$^4F_{5/2} + {}^2H_{9/2}$ (8)	775.2, 793.2, 796.4, 797.8, 798.5, 801.4	774.4, 781.3, 784.8, 792.8, 798.2, 799.0, 800.8	774.4, 780.8, 784.1, 792.4, 797.8, 798.8, 800.4
$^4F_{3/2}$ (2)	864.1, 868.1, 870.4, 876.1,	864.2, 868.0, 870.0, 876.0	864.0, 869.8

reported in the literature [11, 12]. The wavelengths of the components of the 10 K spectra are reported in table 1. These are inhomogeneously broadened even at low temperature. The full width at half-maximum (FWHM) of the most intense features ranges from 20 to 45 cm^{-1}. It is an intermediate value between that typical for crystals (10 cm^{-1}) and for glasses (100 cm^{-1}). In our opinion, this broadening is mainly connected to the structural modulation of these compounds that introduces, as a matter of fact, a disorder in the orientation and/or shape of the coordination polyhedra. The bands in the π polarized spectra are generally more intense than in the σ ones. The structures of the manifolds do not change significantly on passing from one compound to another, allowing us to infer similar oxygen environments around the optically active ions. In the 298 K spectra the components of the manifolds broaden and

Table 2. Experimental and calculated oscillator strengths for BNdLN and Nd:BKN. The Judd–Ofelt parameters, Ω_λ, the RMS and the per cent error are also tabulated.

	BNdLN			Nd:BKN		
Excited state	Barycentre (cm^{-1})	P_{exp} (10^6)	P_{calc} (10^6)	Barycentre (cm^{-1})	P_{exp} (10^6)	P_{calc} (10^6)
$^4F_{3/2}$	11 458	1.37	1.51	11 465	3.08	3.60
$^4F_{5/2} + {}^2H_{9/2}$	12 518	6.61	6.93	12 535	15.8	15.3
$^4F_{7/2} + {}^4S_{3/2}$	13 503	8.24	8.15	13 502	17.2	17.6
$^4F_{9/2}$	14 704	0.81	0.61	14 743	1.32	1.32
$^4G_{5/2} + {}^2G_{7/2}$	17 194	19.1	19.2	17 205	36.3	36.3
$^4G_{9/2} + {}^4G_{7/2} + {}^2K_{13/2}$	19 263	5.68	4.38	19 225	9.51	9.33
$^4G_{11/2} + {}^2G_{9/2} + {}^2K_{15/2} + {}^2(D, F)_{3/2}$	21 329	1.30	1.05	21 394	2.53	2.38
$^2P_{1/2}$	23 230	0.34	0.31	23 181	0.77	0.78
	$\Omega_2 = 3.10 \times 10^{-20}$ cm^2			$\Omega_2 = 5.32 \times 10^{-20}$ cm^2		
	$\Omega_4 = 1.30 \times 10^{-20}$ cm^2			$\Omega_4 = 3.27 \times 10^{-20}$ cm^2		
	$\Omega_6 = 3.19 \times 10^{-20}$ cm^2			$\Omega_6 = 6.87 \times 10^{-20}$ cm^2		
	RMS $= 0.67 \times 10^{-6}$			RMS $= 0.37 \times 10^{-6}$		
	Per cent error $= 11.4$			Per cent error $= 3.8$		

Table 3. Calculated spontaneous emission probabilities A, branching ratios β and radiative lifetime τ for the $^4F_{3/2}$ multiplet of BNdLN and Nd:BKN.

	BNdLN		Nd:BKN	
Final state	A (s^{-1})	β	A (s^{-1})	β
$^4I_{15/2}$	37.7	0.007	81.5	0.007
$^4I_{13/2}$	7.19×10^2	0.127	1.55×10^3	0.128
$^4I_{11/2}$	3.71×10^3	0.559	6.63×10^3	0.545
$^4I_{9/2}$	1.75×10^3	0.308	3.89×10^3	0.320
τ (μs)	176		82	

collapse, giving rise to broad bands. The 800 nm system is the most important absorption channel for laser diode excitation. Its broadness, of about 20 nm ($\sim$270 cm^{-1}), implies a good matching with the pumping radiation even in the presence of the thermal drift of the diode. The room temperature absorption spectra of BNdLN and Nd:BKN have been analysed in the framework of the JO theory [13, 14]. The JO analysis of the spectra of Nd:BNN has already been reported by Romero *et al* [6]. Eight bands were considered to calculate the intensity parameters Ω_λ ($\lambda = 2, 4, 6$); we did not take into account the $^4I_{9/2} \rightarrow {}^2H_{11/2}$ transition because its intensity is negligible. The experimental oscillator strengths of the transitions were reliably determined by considering the polarization of the bands [15] and fitted on the basis of the JO parametrization scheme after subtraction of the magnetic dipole contribution for the $^4I_{9/2} \rightarrow {}^2H_{9/2}$, $^4I_{9/2} \rightarrow {}^4F_{9/2}$, $^4I_{9/2} \rightarrow {}^2G_{7/2}$ and the $^4I_{9/2} \rightarrow {}^2I_{11/2}$ transitions. These contributions are small and not reported here. The reduced matrix elements were taken from Kaminskii [12] and the value of the refractive index was assumed to be $n = 2.33$ [3]. The calculated oscillator strengths, the intensity parameters, the root mean square deviation (RMS) and the per cent error are reported in table 2. The calculated spontaneous emission probabilities and the radiative branching ratios for the transitions from the $^4F_{3/2}$ state to the components of the ^4I_J ($J = 15/2, 13/2, 11/2, 9/2$) manifold are reported in table 3, together with the radiative lifetime of the emitting level. They were estimated using the calculated intensity parameters

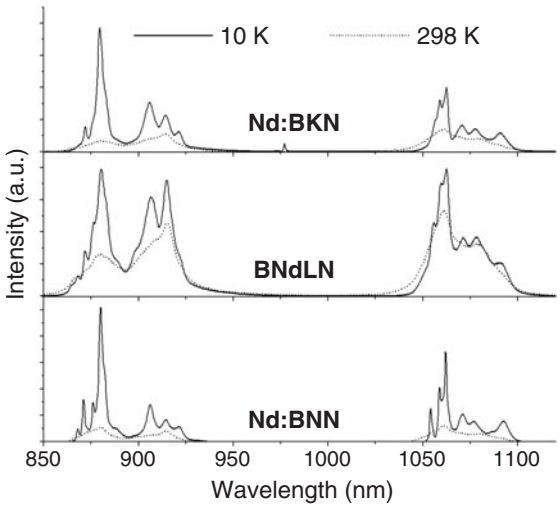

Figure 4. 10 and 298 K emission spectra of Nd:BNN(dil.), BNdLN and Nd:BKN. Excitation wavelength: 514 nm.

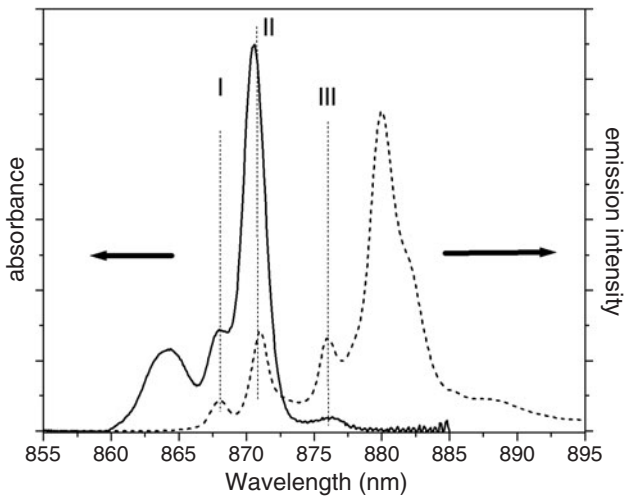

Figure 5. Comparison between the 10 K absorption and emission manifolds of Nd:BNN in the 870 nm region.

and the reduced matrix elements published by Kaminskii [12] and correcting for the refractive index. The obtained parameters are of the same order of magnitude as those reported for Nd:BNN [6] and for the most important laser materials based on the Nd^{3+} ion [11, 12].

The 10 and 298 K emission spectra in the 900 nm and 1 μm regions have been measured after excitation at 514 nm and are shown in figure 4. They correspond to the transitions from the $^4F_{3/2}$ excited level to the $^4I_{9/2}$ and $^4I_{11/2}$ states, respectively. The number of features composing the low temperature spectra indicates the presence of nonequivalent optically active ions. In particular, the comparison between the 10 K $^4F_{3/2} \leftrightarrow {}^4I_{9/2}$ absorption and emission bands of Nd:BNN (figure 5) shows three coincident lines, corresponding to as many different Nd^{3+} centres. FLN measurements extended to the 900 nm region would be useful in order to

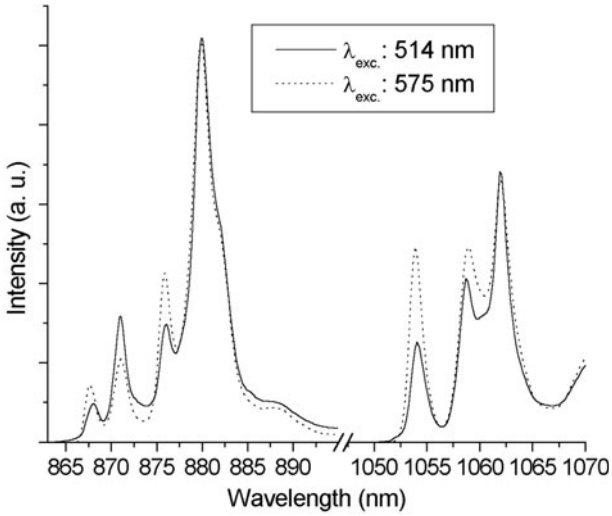

Figure 6. Details of the 10 K emission spectra of Nd:BNN measured at different excitation wavelengths.

characterize these centres but unfortunately this technique is not available in our laboratory. Anyway, we have found it interesting to observe the relative behaviour of the emission lines after excitation at 514 (laser) and 575 nm (filtered Xe lamp), where different centres are preferentially excited. The spectra, shown in figure 6, have been normalized with respect to the most intense feature at 879.9 nm. It can be noted that the relative intensities of the lines at 867.7, 875.9, 1053.9 and 1058.9 nm are lower in the spectrum excited at 514 nm than in that excited at 575 nm, whereas that of the 871.1 nm line is higher and that of the 1061.9 line remains nearly constant, behaving like the reference peak. Site-selective decay curve measurements carried out by Foulon *et al* [16] yielded decay times of 290 and 180 μs for the first and second components of the 1060 nm emission system, respectively, which were assigned to at least two Nd^{3+} centres. Since the second and third components of this system have different behaviours when the excitation wavelength changes, they can be assigned to different centres, confirming the presence of three nonequivalent optically active ions. The nature of these different centres has to be consistent with the site occupancy reported in the previous section. Since each A_2 site is surrounded by four A_1 sites (see figure 1, where the out-of-plane ions are at longer distances) and these are not fully occupied, there are finite probabilities of having one or two Ba^{2+} vacancies in the second coordination sphere of Nd^{3+}. The presence or absence of vacancies implies different charge distributions around the active ions and it is more than sufficient to generate nonequivalent optical centres. In order to support (or reject) this hypothesis, we have measured also the 10 and 298 K emission spectra of Nd:BLN, a crystal whose structure, in comparison to the TTB one, presents the same 15-fold A_1 site but a different 12-fold site (A_3 instead of A_2), as discussed in the previous section. They are shown in figure 7. The evident difference in these spectra from those of the other niobates clearly indicates a different crystal field geometry for the luminescent centres, according to the site occupancy data obtained from XRD measurements. We can then reasonably suppose that in the TTB structure the nonequivalent active ions are composed of Nd^{3+} ions located in A_2 sites with no, one or two Ba^{2+} vacancies in the second coordination sphere. The room temperature decay curve of Nd:BLN is a single exponential, that of Nd:BNN(dil.) is nearly single exponential,

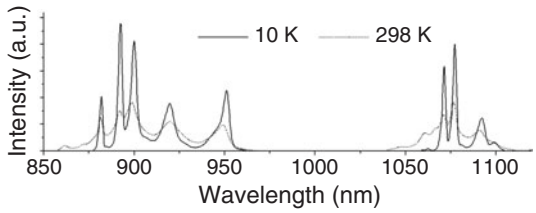

Figure 7. 10 and 298 K emission spectra of Nd:BLN.

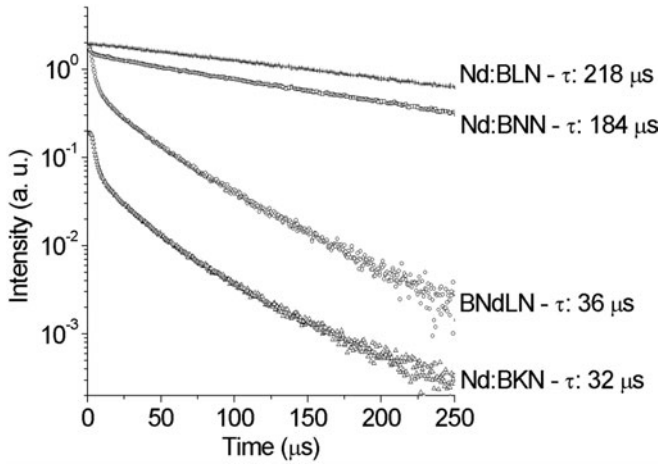

Figure 8. Room temperature decay curves of Nd:BLN, Nd:BNN, BNdLN and Nd:BKN, obtained after pulsed excitation at 740 nm.

whereas those of BNdLN and Nd:BKN are clearly not exponential, indicating the presence of short range interactions between the Nd^{3+} ions in the two more concentrated systems. In these cases attempts to fit the decay profiles using equations based on known energy transfer models have failed and the decay times have been estimated by considering the long time tails of the curves. These results are summarized in figure 8. Comparison between the experimental decay times of BNdLN and Nd:BKN and their radiative lifetimes calculated by means of JO theory indicates that nonradiative processes are active. In our opinion these are energy transfer processes whose dependence on the temperature and Nd^{3+} concentration will be investigated in the future in order to assess the best operating conditions for these materials.

5. Conclusions

Nd:BNN, BNdLN and Nd:BKN solid solutions with the TTB structure have been grown in the form of single crystals using the 'flux growth' technique and their optical spectra have been measured at 10 and 298 K. The low temperature spectra indicate the presence of three main nonequivalent optical centres, whose nature has been discussed on the basis of the structural information and of the comparison with the spectra of Nd:BLN. Our experimental evidence leads to conclusions different from those of Foulon *et al* [4, 16], who supposed that the Nd^{3+} ions replace both Na^{+} and Ba^{2+} on the basis of site-selective spectroscopic measurements. Therefore the site occupancy of the active ions in these materials has to be considered still an open question and needs further experimental work in order to be fully understood. The

inhomogeneous broadening of components of the observed manifolds is mostly due, in our opinion, to the structural modulation affecting these crystals. The room temperature spectra are composed of very broad bands which make these materials interesting candidates for diode pumped and tunable solid state laser operation. JO theory has been applied to analysis of the 298 K absorption spectra of BNdLN and Nd:BKN, yielding intensity parameters of the same order of magnitude as for other Nd^{3+}-based laser crystals. The difference between the calculated radiative lifetimes and the experimental decay times of these compounds has been ascribed to energy transfer processes connected to the relatively high concentration of active ions. In a forthcoming paper we will give detailed information on the crystal growth procedure and on the crystallographic properties of these materials. The work will then be extended to other new TB phases and to crystals containing optically active ions different from Nd^{3+}.

Acknowledgments

This work was supported by the Ministero dell'Istruzione, dell'Università e della Ricerca (project COFIN 2001). The authors acknowledge Mrs Paola Copelli for her assistance in the crystal growth experiments and Professor Marco Bettinelli (Università di Verona) for helpful discussions.

References

[1] Neurgaonkar R R and Cory W K 1986 *J. Opt. Soc. Am.* B **3** 274
[2] Singh S, Draegert D A and Geusic J E 1970 *Phys. Rev.* B **2** 2709
[3] Kaminskii A A, Koptsik V A, Maskaev Y A, Naumova I I, Rashkovich L N and Sarkisov S E 1975 *Phys. Status Solidi* a **28** K5
[4] Foulon G, Brenier A, Ferriol M, Cohen-Adad M T and Boulon G 1996 *Chem. Phys. Lett.* **249** 381
[5] Lebbou K, Itagaki H, Yoshikawa A, Fukuda T, Carrillo-Romo F, Boulon G, Brenier A and Cohen-Adad M T 2000 *J. Cryst. Growth* **210** 655
[6] Romero J J, Brenier A, Bausà L E, Boulon G, Garcia Solé J and Kaminskii A A 2001 *Opt. Commun.* **191** 371
[7] Altomare A, Burla M C, Camalli M, Cascarano G L, Giacovazzo C, Guagliardi A, Moliterni A, Polidori G and Spagna R 1999 *J. Appl. Crystallogr.* **32** 115
[8] Sheldrick G M 1997 *SHELX-97, Program for the Refinement of Crystal Structures* University of Goettingen, Germany
[9] Labbé Ph, Leligny H, Raveau B, Schneck J and Toledano J C 1989 *J. Phys.: Condens. Matter* **2** 25
[10] Schneck J and Denoyer F 1981 *Phys. Rev.* B **23** 383
[11] Kaminskii A A 1981 *Laser Crystals* 2nd edn (Berlin: Springer)
[12] Kaminskii A A 1996 *Crystalline Lasers: Physical Processes and Operating Schemes* (Boca Raton, FL: CRC Press)
[13] Judd B R 1962 *Phys. Rev.* **127** 750
[14] Ofelt G S 1962 *J. Chem. Phys.* **37** 511
[15] Lomheim T S and DeShazer L G 1978 *J. Appl. Phys.* **49** 5517
[16] Foulon G, Ferriol M, Brenier A, Cohen-Adad M T, Boudeulle M and Boulon G 1997 *Opt. Mater.* **8** 65